ANKARA YILDIRIM BEYAZIT UNIVERSITY

GRADUATE SCHOOL OF NATURAL AND APPLIED SCIENCES

INVESTIGATION OF HOT FORGED CHARACTERISTICS OF INCONEL 718

M.Sc. Thesis by

Bengisu BAYRAKTAR

Department of Materials Engineering

August, 2024

ANKARA

INVESTIGATION OF HOT FORGED CHARACTERISTICS OF INCONEL 718

A Thesis Submitted to

The Graduate School of Natural and Applied Sciences of

Ankara Yıldırım Beyazıt University

In Partial Fulfillment of the Requirements for the Degree of Master of Science

in Materials Engineering, Department of Metallurgy and Materials Engineering

by

Bengisu BAYRAKTAR

August, 2024

ANKARA

M.Sc. THESIS EXAMINATION RESULT FORM

We have read the thesis entitled "**INVESTIGATION OF HOT FORGED CHARACTERISTICS OF INCONEL 718**" completed by **BENGİSU BAYRAKTAR** under the supervision of **PROF. DR. GÜVEN ÇANKAYA** and we certify that in our opinion it is fully adequate, in scope and in quality, as a thesis for the degree of Master of Science.

Prof. Dr. Güven ÇANKAYA

Supervisor

Assoc. Prof. Dr. Mehmet Fatih ÖKTEM

Jury Member

Prof. Dr. Hakan ATEŞ

Jury Member

Prof. Dr. Sadettin ORHAN

Director

Graduate School of Natural and Applied Sciences

ETHICAL DECLARATION

I hereby declare that, in this thesis which has been prepared in accordance with the Thesis Writing Manual of Graduate School of Natural and Applied Sciences,

- All data, information and documents are obtained in the framework of academic and ethical rules,
- All information, documents and assessments are presented in accordance with scientific ethics and morals,
- All the materials that have been utilized are fully cited and referenced,
- No change has been made on the utilized materials,
- All the works presented are original,

and in any contrary case of above statements, I accept to renounce all my legal rights.

Date: 2024, August **Signature: ……..**

Name & Surname: Bengisu BAYRAKTAR

ACKNOWLEDGMENTS

First and foremost, I would like to express my deepest gratitude to my advisor, Prof. Dr. Güven ÇANKAYA, for his patience, extensive knowledge, and encouragement throughout my graduate studies and research. His belief in me and my work during both my undergraduate and graduate studies made it possible for me to complete my education.

I would also like to extend my heartfelt thanks to my former employer, Parsan, which provided me with invaluable learning experiences and lessons, and to Gürbüz GÜZEY for giving me the opportunity to work on this thesis topic and for offering the necessary resources.

I owe special thanks to my family for their boundless support and understanding during challenging times. Without them, I could not have achieved this.

Lastly, I would like to express my gratitude to all my colleagues and everyone who contributed, directly or indirectly, to the completion of this thesis, especially to Aysu Hande YÜCEL for her unwavering support and assistance.

2024, 12 August **Bengisu BAYRAKTAR**

INVESTIGATION OF HOT FORGED CHARACTERISTICS OF INCONEL 718

ABSTRACT

This thesis explores the effects of hot forging on the microructure and mechanical properties of Inconel 718, a nickel-based superalloy extensively used in high-temperature environments, such as aerospace, power generation, and chemical processing. Inconel 718 is recognized for its exceptional strength, corrosion resistance, and stability at elevated temperatures, making it an ideal material for critical components exposed to extreme conditions.

The study systematically investigates how hot forging, a process carried out above the alloy's recrystallization temperature, influences the grain structure, phase distribution, and mechanical characteristics of Inconel 718. Using advanced techniques such as scanning electron microscopy, energy dispersive spectroscopy, and X-Ray diffraction, the research provides a comprehensive analysis of the microstructural evolution and identifies key changes that occur during the forging process. The mechanical properties, including tensile strength, ductility, and stress rupture behavior, are examined through rigorous testing at both room and elevated temperatures.

One of the critical findings of the study is the identification of optimal forging parameters that result in desirable microstructural features, such as grain refinement and phase uniformity, which are crucial for enhancing the alloy's mechanical performance. The research also emphasizes the role of post-forging heat treatments in further improving the material’s properties, particularly in achieving a balance between strength and ductility.

The thesis provides practical recommendations for optimizing the hot forging and heat treatment processes to achieve superior performance in Inconel 718 components. These recommendations are aimed at improving the material’s reliability and durability in demanding industrial applications.

Keywords: Inconel 718, hot forging, microstructure, mechanical properties, heat treatment.

INCONEL 718'IN SICAK DÖVME ÖZELLIKLERININ İNCELENMESI

ÖZ

Bu tez, sıcak dövmenin Inconel 718'in mikro yapısı ve mekanik özellikleri üzerindeki etkilerini incelemektedir. Inconel 718, havacılık, enerji üretimi ve kimyasal işlem gibi yüksek sıcaklık ortamlarında yaygın olarak kullanılan bir nikel bazlı süper alaşımdır. Inconel 718, olağanüstü mukavemeti, korozyon direnci ve yüksek sıcaklıklardaki stabilitesi ile tanınır ve aşırı koşullara maruz kalan kritik bileşenler için ideal bir malzemedir.

Çalışma, sıcak dövmenin, alaşımın rekristalizasyon sıcaklığının üzerinde gerçekleştirilen bir işlem olarak, Inconel 718'in tane yapısını, faz dağılımını ve mekanik özelliklerini nasıl etkilediğini sistematik olarak araştırmaktadır. taramalı elektron mikroskobu, enerji dağılımlı spektroskopi ve X-Işını difraksiyonu gibi ileri teknikler kullanılarak, mikro yapısal evrimin kapsamlı bir analizi sağlanmakta ve dövme süreci sırasında meydana gelen önemli değişiklikler belirlenmektedir. Mekanik özellikler, çekme mukavemeti, süneklik ve gerilme kopma davranışı da hem oda sıcaklığında hem de yüksek sıcaklıklarda yapılan titiz testlerle incelenmiştir.

Çalışmanın önemli bulgularından biri, alaşımın mekanik performansını artırmada kritik olan tane inceltmesi ve faz homojenliği gibi istenen mikro yapısal özellikleri sağlayan optimal dövme parametrelerinin belirlenmesidir. Araştırma ayrıca, malzemenin özelliklerini daha da iyileştirmede, özellikle mukavemet ve süneklik arasında bir denge sağlamada, dövme sonrası ısıl işlemlerin rolünü vurgulamaktadır.

Bu tez, Inconel 718 bileşenlerinde üstün performans elde etmek için sıcak dövme ve ısıl işlem süreçlerini optimize etmeye yönelik pratik öneriler sunmaktadır. Bu öneriler, malzemenin zorlu endüstriyel uygulamalardaki güvenilirliğini ve dayanıklılığını artırmayı hedeflemektedir.

Anahtar Kelimeler: Inconel 718, sıcak dövme, mikro yapı, mekanik özellikler, ısıl işlem.

CONTENTS

NOMENCLATURE

Roman Letters Symbols

A	Area, m^2
Cp	Specific heat at constant pressure, J/kg·K
E	Modulus of elasticity, GPa
F	Force, N
G	Shear modulus, GPa
H	Enthalpy, J
K	Thermal conductivity, W/m·K
L	Length, m
M	Mass, kg
N	Number of cycles
P	Pressure, MPa
Q	Heat, J
R	Universal gas constant, J/mol·K
S	Entropy, J/K
T	Temperature, °C
U	Internal energy, J
V	Volume, m^3
W	Work, J
X	Mole fraction

Greek Letters Symbols

α	Coefficient of thermal expansion, 1/°C
β	Coefficient of thermal conductivity, W/m·K
δ	Thickness, mm
ε	Strain
γ	Surface tension, N/m
κ	Thermal diffusivity, m^2/s
λ	Wavelength, m
μ	Dynamic viscosity, Pa·s
ν	Poisson's ratio
ρ	Density, kg/m^3

σ	Stress, MPa
τ	Shear stress, MPa

Subscripts

c	Cold side
f	Fin
h	Hot side
i	Initial
m	Mean
max	Maximum
min	Minimum
1, 2	Inlet and Outlet

Acronyms

BDC	Bottom Dead Center
EDS	Energy Dispersive Spectrometry
SEM	Scanning Electron Microscopy
XRD	X-Ray Diffraction
IN718	Inconel 718

LIST OF TABLES

LIST OF FIGURES

CHAPTER 1

INTRODUCTION

Inconel 718 is a high-strength, corrosion-resistant nickel-chromium alloy widely utilized in high-temperature applications such as aerospace, power generation, and chemical processing industries. Its unique combination of properties, including excellent creep resistance, oxidation resistance, and weldability, makes it an ideal choice for components subjected to extreme environments. Hot forging plays a critical role in the manufacturing of Inconel 718 components as it significantly affects the microstructural evolution and mechanical properties of the material. During hot forging, the alloy undergoes plastic deformation at elevated temperatures, resulting in grain refinement, dissolution of precipitates, and the development of desirable textures. These microstructural changes are crucial in determining the final performance characteristics of the forged component [1-3].

This study aims to systematically explore the effects of hot forging on the microstructure and mechanical properties of Inconel 718. Understanding the relationship between processing parameters and the resulting material characteristics enables the optimization of the forging process to achieve superior performance in demanding applications. This research involves a comprehensive analysis of microstructural features, such as grain size, phase distribution, and the presence of any defects or inclusions, using advanced characterization techniques like Scanning Electron Microscopy (SEM). Additionally, the study evaluates the mechanical properties, including tensile strength, hardness, and fatigue resistance, to assess the impact of hot forging on the alloy's performance.

The findings from this study are anticipated to offer valuable insights into optimizing the forging processes for Inconel 718, thereby contributing to the development of more efficient and reliable high-temperature components.

1.1 Objectives of This Study

The purpose of this thesis, as suggested by the title 'Investigation of Hot Forged Characteristics of Inconel 718' is to explore the microstructure and mechanical properties of Inconel 718 after the hot closed-die forging process. The study aims to identify the changes in microstructure and mechanical properties resulting from the forging process and understand how these changes impact the material's overall performance. Furthermore, the thesis seeks to optimize the forging process parameters and heat treatment procedures to achieve the desired properties for specific applications. Ultimately, the objective is to enhance the understanding of Inconel 718's behavior post-hot closed-die forging and provide recommendations for improving its properties across various applications.

1.2 Outline of the Thesis

In this thesis, information about the literature review of Inconel 718 materials is provided in Chapter 2. Chapter 3 discusses the production and characterization methods used in this study, while Chapter 4 describes the tests conducted to gather information on Inconel 718. The results of these tests and their discussions are presented in Chapter 5. Finally, Chapter 6 offers conclusions drawn from this study and suggests directions for future research.

CHAPTER 2

LITERATURE REVIEW

2.1 Superalloys

Superalloys, which are a class of materials designed for exceptional mechanical strength, high-temperature stability, and resistance to corrosion and wear, are primarily used in components that must perform under high heat, such as in gas turbine engines. These alloys typically consist of nickel, nickel-iron, or cobalt, and are known for their durability in extreme condition [4].

Superalloys are typically composed of a combination of base metals, such as iron, cobalt, or nickel, along with alloying elements such as chromium, molybdenum, and tungsten. These elements impart unique properties to the alloy, such as high-temperature strength, corrosion resistance, and thermal stability. The resulting alloys can withstand high mechanical and thermal loads, making them suitable for extreme environments [5,6].

Superalloys are manufactured using a range of techniques, including casting, forging, and powder metallurgy. Casting is the most common method of producing superalloys, wherein the molten metal is poured into a mold and allowed to solidify. Forging involves the deformation of the metal under high pressure, while powder metallurgy involves the consolidation of metal powders using heat and pressure Due to their excellent properties, superalloys are utilized in various applications at both room and high temperatures, such as rocket components, nuclear reactors, industrial furnaces, heat exchangers, petrochemical equipment, petroleum production equipment, automotive turbochargers, and biomedical devices. Specifically, in aircraft and industrial gas turbine components, superalloys are used to make disks, bolts, shafts, cases, blades, and vanes. Additionally, superalloys find applications in hot work tools and dies, casting dies, dentistry devices, trays, fixtures, conveyor belts, and nuclear power systems [6,7].

In conclusion, superalloys are a critical class of materials that possess exceptional mechanical and thermal properties, enabling them to operate under harsh and demanding conditions. They are utilized in various industries, including aerospace, power generation, chemical processing, and medical implants, catering to diverse application-specific requirements.

2.1.1 Nickel-Based Superalloys

Nickel-based superalloys, specifically, are engineered for environments where conventional metals would fail. Their unique composition, often including elements such as chromium, cobalt, and molybdenum, allows them to maintain structural integrity at high temperatures, making them indispensable in industries like aerospace and power generation [7,8].

Nickel-based superalloys are typically composed of nickel, along with alloying elements such as chromium, cobalt, molybdenum, tungsten, and aluminum. These elements impart unique properties to the alloy, such as high-temperature strength, corrosion resistance, and thermal stability. The resulting alloys can withstand high mechanical and thermal loads, making them suitable for use in extreme environments. Nickel-based superalloys are manufactured using a range of techniques, including casting, forging, and powder metallurgy. Casting is the most common method of producing nickel-based superalloys, wherein the molten metal is poured into a mold and allowed to solidify. Forging involves the deformation of the metal under high pressure, while powder metallurgy involves the consolidation of metal powders using heat and pressure [7,9].

Nickel-based superalloys are utilized in various applications, including aerospace turbine engines, power generation turbines, and chemical processing reactors. Chemical processing reactor is shown in Figure 2.1. In aerospace, nickel-based superalloys are used to manufacture critical engine components, such as turbine blades, discs, and shafts, which require high strength and high-temperature stability. In power generation, nickel-based superalloys are used to manufacture gas turbine blades and vanes, which require high-temperature strength and corrosion resistance.

In chemical processing, nickel-based superalloys are used to manufacture equipment exposed to aggressive chemicals and high-temperature environments [10,11].

In conclusion, nickel-based superalloys are a class of high-performance materials that exhibit exceptional mechanical strength, high-temperature stability, and excellent resistance to corrosion and wear. These alloys are widely utilized in various critical applications due to their unique properties and capabilities. Nickel-based superalloys have the highest thermal resistance and strength among all superalloys. Due to these fundamental advantages, they are considered the optimal material for many challenging applications. Examples of areas where nickel-based superalloys are used include applications such as turbine disks and turbine blades [10,12].

Figure 2.1 Chemical processing reactor

2.1.2 Inconel 718

Inconel 718, a nickel-based superalloy, is extensively used across various industries, thanks to its exceptional high-temperature strength, corrosion and oxidation resistance, and fatigue durability. It is engineered to perform under extreme conditions, making it ideal for critical applications in sectors such as aerospace, power generation, and chemical processing [13].

The alloy's composition, which includes elements like chromium, molybdenum, niobium, and iron, imparts it with remarkable mechanical and thermal properties.

These properties enable Inconel 718 to withstand intense mechanical and thermal stress while maintaining resistance to corrosion and oxidation, even in aggressive environments.

Inconel 718 is manufactured through several techniques, most commonly casting, where the molten alloy is shaped in a mold and solidified. Forging, which involves deforming the metal under high pressure, and powder metallurgy, which consolidates metal powders through heat and pressure, are also used to produce this alloy.

The alloy is utilized in various critical applications in aerospace, power generation, and chemical processing. In aerospace, Inconel 718 is used to manufacture critical engine components such as turbine blades and discs, which require high strength and high-temperature stability. In power generation, Inconel 718 is used to manufacture gas turbine components, which require high-temperature strength and corrosion resistance. In chemical processing, Inconel 718 is used to manufacture equipment exposed to aggressive chemicals and high-temperature environments. Nickel based superalloy positions in a jet engine are shown in Figure 2.2. [14,15].

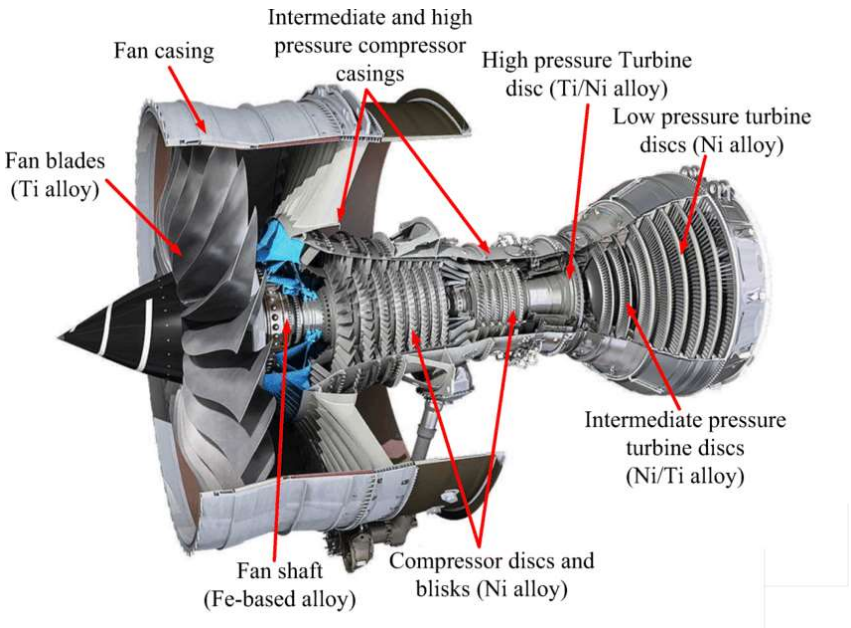

Figure 2.2 Nickel based superalloy positions in a jet engine

Inconel 718 is used in a variety of critical applications across various industries. Some of the key applications of Inconel 718 include: aerospace, where it is utilized in the manufacture of critical engine components such as turbine blades, discs, and casings due to its high-temperature strength, corrosion and oxidation resistance, and fatigue resistance; power generation, where it is employed in gas turbine components like combustion liners, transition ducts, and high-pressure turbine blades because of its suitability for high-temperature and corrosive environments; chemical processing, where it is used in equipment such as reactors, heat exchangers, and valves exposed to aggressive chemicals and high temperatures; and oil and gas, where it is found in downhole tools like drill collars and subsea equipment such as valves and connectors due to its high strength and corrosion resistance in harsh and corrosive environments [16,17].

In summary, Inconel 718 is a versatile material that is used in various critical applications across industries, where its unique combination of properties, including high-temperature strength, corrosion and oxidation resistance, and fatigue resistance, make it a suitable choice for use in harsh and demanding environments.

2.2 Forging

Forging is an essential metalworking process widely used for manufacturing high-performance, reliable components. This technique involves applying compressive forces to deform and shape metals in their solid state, offering several advantages that make it indispensable across various industries. One of the key benefits of forging is the refinement of the metal's grain structure, which is aligned with the final product's contours. This refinement leads to enhanced mechanical properties such as strength, toughness, and ductility, making forged components ideal for severe loading conditions. Forged parts also exhibit superior structural integrity compared to those that are cast or machined. The forging process eliminates internal voids, inclusions, and other defects, which can compromise a component's performance and reliability under demanding operational environment. Forging allows for the manufacturing of components with consistent dimensions and minimal variability between different production runs. This uniformity enables the cost-effective production of large

quantities of high-quality parts. Due to the refined grain structure and the absence of internal defects, forged components display increased resistance to fatigue failure. This characteristic is particularly important for parts exposed to cyclic loading or stress concentrations. Forging offers a high degree of flexibility in design and production, accommodating the manufacture of complex and unique geometries tailored to specific applications [18-24].

2.2.1 Hot Forging

Hot forging is a metalworking process performed at temperatures above the metal's recrystallization point, which softens the metal and enhances its malleability, thereby reducing the force needed for plastic deformation. Once softened, the metal is shaped into the desired form using high pressure, typically applied via a press or hammer [25].

This process offers significant advantages over other metalworking methods, particularly in its ability to produce complex and intricate shapes that would be difficult to achieve otherwise. Additionally, the high pressure involved in hot forging results in components with refined grain structures and enhanced mechanical properties such as strength, ductility, and toughness. Additionally, hot forging can produce components with minimal surface porosity and internal defects, ensuring greater structural integrity and performance reliability. This process is particularly useful for the production of safety-critical components, such as aircraft landing gear, engine components, and automotive suspension parts. The hot forging process is illustrated in Figure 2.3.

Figure 2.3 Image of hot forging from our process

Hot forging is widely utilized across various industries, including automotive, aerospace, construction, and energy. It is particularly suitable for manufacturing parts that require high strength, durability, and performance, catering to a diverse range of application-specific requirements [26-29].

2.2.2 Closed Die Forging

Closed die forging is a process where metal is deformed within a set of dies that completely enclose it, making it ideal for producing high-precision components with complex geometries. This technique combines compressive forces and controlled material flow to shape the metal precisely. As a result, the components produced through closed die forging have refined grain structures, enhanced mechanical properties, and minimal surface porosity or internal defects [30,32].

As illustrated in Figure 2.4, closed die forging involves deforming a workpiece between two dies that fully enclose it, with the material being stamped until the desired shape is achieved [32].

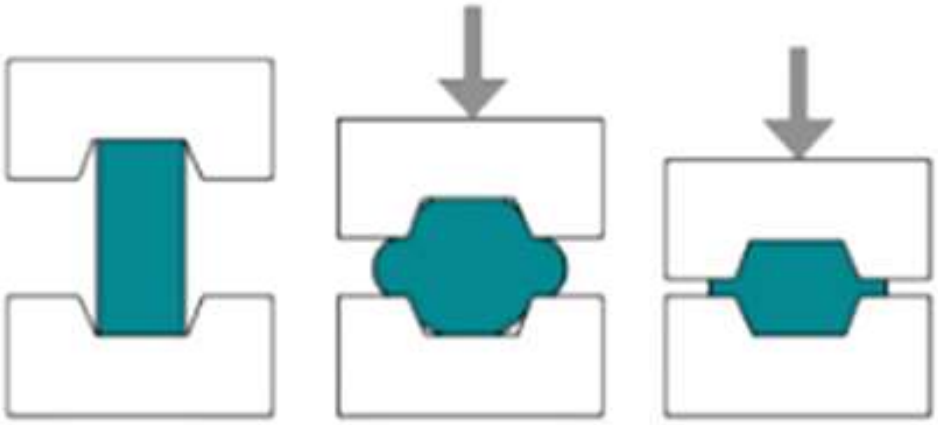

Figure 2.4 Closed die forging is the process

CHAPTER 3

METHODOLOGY

3.1 Materials

The experimental part of this study focuses on the forging methods applied to Inconel 718. The raw material used in these processes was Inconel 718. The composition and properties of the alloy, supplied by Böhler, are detailed in Table 3.1. Additional details, apart from the composition, cannot be disclosed due to the company's confidentiality policy.

Table 3.1 Chemical composition of the Inconel 718

Element	C	Si	Mn	P	S
Composition (%)	0.02400	0.06000	0.07000	0.00600	0.00050
Element	Cr	Mo	Ni	Cu	Co
Composition (%)	17.92000	2.98000	53.90000	0.05000	0.32000
Element	Ti	Al	Nb	B	Fe
Composition (%)	0.90000	0.49000	5.19000	0.00280	18.04000
Element	N	Pb	Ta	O	Bi
Composition (%)	0.00400	<0.00030	<0.02000	0.00050	<0.00003
Element	Ca	Mg	Sn	Se	Ag
Composition (%)	<0.00020	0.00100	<0.00100	<0.00030	<0.00010

3.2 Forging Production

During the forging process of Inconel 718, the temperature across the entire part, from the moment it exits the furnace until it reaches its final shape, must be maintained between 950°-1050°C, excluding the machining allowance/drilled hole. Additionally, the strain rate must not exceed 10 s^{-1}. To achieve the desired values, process optimization was conducted using Finite Element Analysis (FEA) simulations.

As depicted in Figure 3.1, simulations for the Inconel 718 material, considering the deformation rate and process temperature (950-1050°C) along with an annealing temperature of 1000°C, suggested that the forging process should be performed using a 12800-ton screw press at 100% energy, with a pancake geometry at an annealing temperature of 1000°C. The brand of the press cannot be disclosed due to company policy. As shown in Figure 3.2, the material was forged at temperatures between 950°-1050°C following annealing at 1000°C. Figure 3.3 illustrates the material after the forging process.

Heat treatment involves a series of heating and cooling processes applied to the material to ensure that its structure and mechanical properties meet the required specifications [33]. After the forging process, necessary analyses were conducted, and the heat treatment parameters for the vacuum furnaces were determined. The heat treatment process is graphically depicted in Figure 3.4.

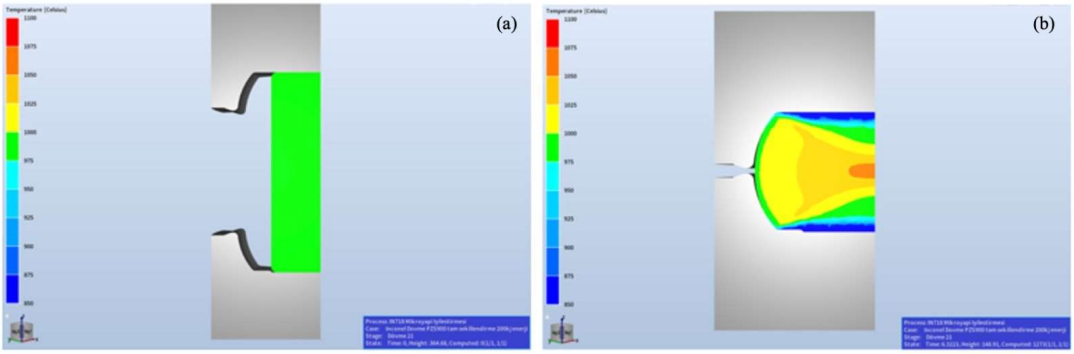

Figure 3.1 Simulation of single-stroke forging (a) initial shape (b) after forging

The solutionizing temperature for all parts is set at 960±14°C. Once the solutionizing temperature decreases to 8°C below the core charge thermocouple temperature, the parts are held for 60 minutes regardless of thickness. Following this, the parts undergo nitrogen gas cooling at a minimum rate of 35°C/min within the temperature range of 500-960°C, continuing until the charge thermocouple temperature drops below 900°C. The first-stage aging temperature is set at 720±8°C for all parts, with a minimum

holding time of 8 hours, beginning when the charge thermocouple reaches the lower tolerance of 712°C. After the first aging stage, the furnace temperature is reduced at a rate of 56°C/hour until it reaches the second aging temperature of 635±8°C. The second aging stage is maintained at 635±8°C, with a minimum holding time of 8 hours, starting when the furnace control thermocouple reaches the upper tolerance of 643°C. Finally, after completing the second aging stage, all parts are cooled under a maximum nitrogen pressure of 3.0 bar, concluding the process once the charge thermocouple temperature drops below 900°C.

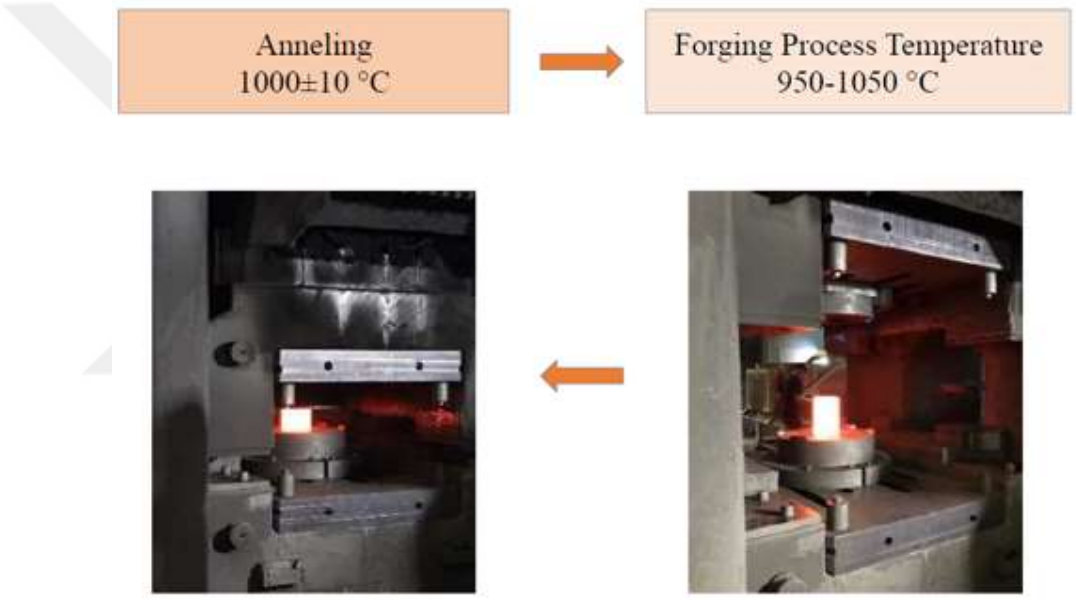

Figure 3.2 Forging process scheme of IN718 alloy

Figure 3.3 IN718 material after forging

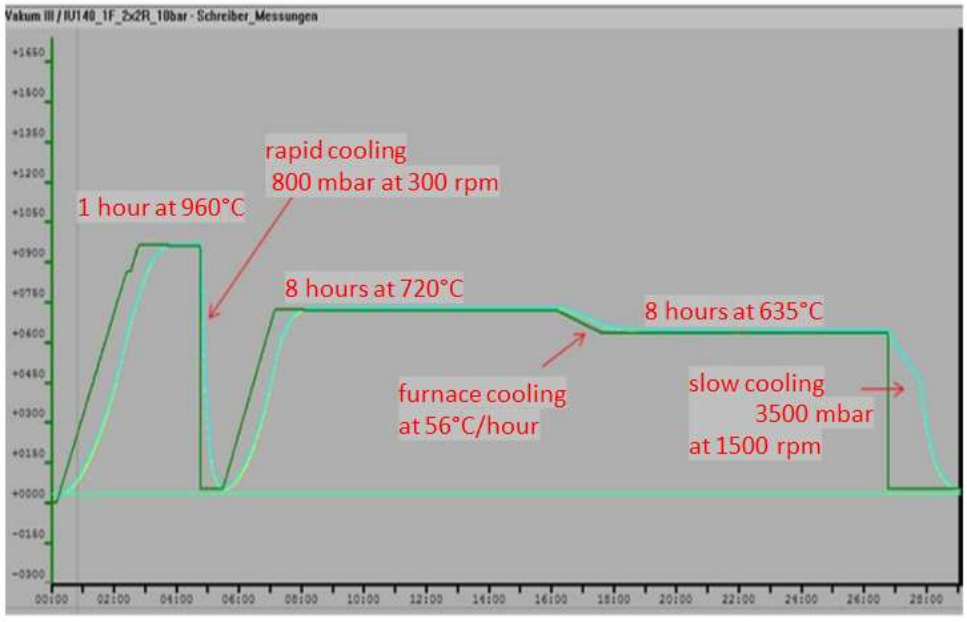

Figure 3.4 Heat treatment process graphic of INC718 alloy

CHAPTER 4

EXPERIMENTAL PROCEDURE

4.1 Macrostructural Analysis

Macro etching was applied by cutting the pieces in half both radially and axially. The macrostructure was evaluated for uniformity and harmful inclusions, which were observed for further microstructural examinations. Grain flow should show no evidence of re-entrant grain flow, buckling, or kinking. The macrostructure should be free from pronounced banding, grain size variation, and detrimental features such as freckles or white spots. The images will be identified as MA-0 and MA-180 for the radial sections of 0º and 180º, respectively. The grain flow of die forgings, except in areas containing flash-line end grain, is expected to follow the general contour of the forging and show no evidence of re-entrant grain flow [34].

After sample preparation, the samples were etched using the immersion method for metallographic examinations. An etching solution consisting of 8.8g FeCl3 + 2.4g CuCl2 + 112 ml HCl + 6 ml HNO3 + 122 ml ethanol was used. Macroscopic images of the samples were captured after the etching process. During macrostructural analysis, examinations were performed using a Nikon AZ100 Stereo Microscope as seen in Figure 4.1.

Figure 4.1 An image of Nikon AZ100 stereo microscope

4.2 SEM – EDS Phase Analysis

In the examination of the samples using scanning electron microscopy (SEM) and energy dispersive X-ray spectroscopy (EDS), the Hitachi Desktop Microscope TM3030 was used.

4.3 XRD Analysis

XRD analysis was conducted to determine the phases present in the microstructure of the Inconel 718 alloy sample. The analysis was performed using the Bragg-Brentano method on a Rigaku XRD instrument, with a copper tube voltage of 45 kV and a current of 200 mA.

4.4 Grain Size Analysis

Suitable metallographic sample preparation procedures were followed for the Inconel 718 alloy samples. After performing the appropriate polishing procedure, the samples were subjected to electrolytic etching, and microstructure images were captured. Subsequently, a total of 12 samples, labeled N1-N3, were analyzed for grain size according to ASTM E112 standards using a microstructural image analyzer on both longitudinal and transverse sections.

For electrolytic etching, a solution of CrO_3 + Na_2SO_4 was used, and a voltage of 10 volts was applied to the samples for a duration of 30 seconds. Microstructure images after etching were captured using an Olympus BX53M optical microscope at various magnifications.

4.5 Ala Grain Size Measurement

According to ASTM E930, the analysis of the largest grain size in ALA can be performed on samples containing coarse grains that deviate from the general microstructure. It is stated that this analysis can also be used to measure average grain size according to ASTM E112, particularly when these coarse grains are sparse throughout the sample due to their rarity compared to the overall microstructure. These coarse grains, which may contribute to crack initiation, propagation, and fatigue

damage, can be analyzed under ASTM E930 if the following conditions are met: the presence of sparse coarse grains in a microstructure with a homogeneously distributed equiaxed grain structure, and these grains having an ASTM grain size number 3 or more larger than the surrounding homogeneous grain sizes. Additionally, the area occupied by the coarse grains should not exceed 5% of the total surface area of the sample.

4.6 Mechanical Tests

Tensile and creep tests were conducted on Inconel 718 superalloy samples. The tensile tests were performed at room temperature according to ASTM E8/E8M, and at 400°C and 650°C according to ASTM E21, using a Zwick 2600 (600kN) Universal Testing Machine.

Tensile test coupons and testing procedures will be in accordance with ASTM E21. Elongation values will be reported as 4D %. A strain rate of 0.005 inch/inch/minute (0.005 mm/mm/minute) will be used until reaching 0.2% yield strength.

Stress rupture test specimens and combination smooth-and-notched specimens are tested according to ASTM E292. A standard cylindrical combination smooth-and-notched specimen conforming to ASTM E292 can be tested following AMS 5663M section 3.5.1.5.1. Results are reported in accordance with AMS 5663 paragraph 3.5.1.5.

CHAPTER 5

RESULT AND DISCUSSION

5.1 Macrostructural Analysis

After macro etching of the MA-1 sample, stress flow lines resulting from the forging process can be observed. There are no visible inclusions or oxide-like structures on the sample surface that could create any discontinuities. However, a streak in the shape of an arc is observed in the region indicated in the image. To provide a clear interpretation, a microstructural examination was performed on a sample prepared from the marked location in the right image, as shown in Figure 5.1.

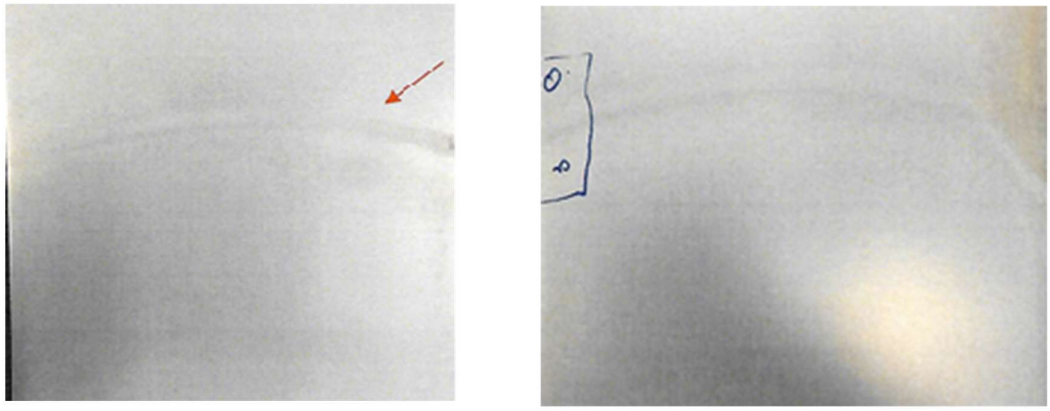

Figure 5.1 Component with visible flow lines on the surface after etching (coded as MA-1)

In the N1 sample, as shown in Figure 5.2, a sample was prepared from the side of the component to investigate the presence of any structures that could create discontinuities propagating into the metal. Upon examination of the microstructural sample prepared from this region, as shown in Figure 5.3. It was observed that there were significantly small equiaxed grains and the presence of small spherical phases. To clarify the phases in the microstructure of this sample, SEM-EDS analysis was conducted. No traces of the streak observed during macro etching were found in the microstructural image analysis of this particular region. The microstructure exhibited a homogeneous structure with equiaxed grains. No discontinuities that could cause

heterogeneity were observed. Therefore, to examine the streak more clearly from the surface, a sample was prepared from the surface of the component, as shown in Figure 5.4.

Figure 5.2 Region where the microstructural sample was prepared

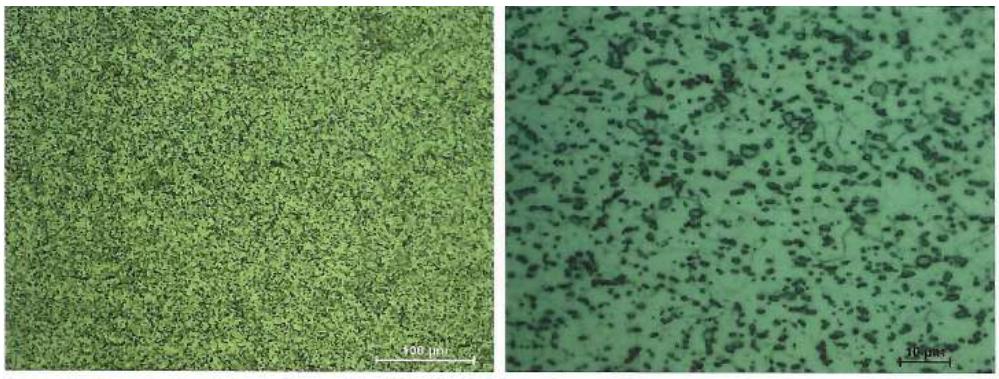

Figure 5.3 The microstructural images of the side section of the macrostructure showing the streak

In the microstructural analysis of the microsample prepared from the surface of the N1 component after macro etching, no formation of any phase or oxide inclusion-like structure causing heterogeneity was observed. The microstructure images shown in Figure 5.5 exhibit the presence of equiaxed small grains and spherical morphology phases. However, during the microstructural examinations, significant segregation of

the mentioned phases was observed in the region where the streak was present on the component. Below, in Figure 5.6, an intermediate surface image shows the regions with dense and less frequent occurrence of these phases.

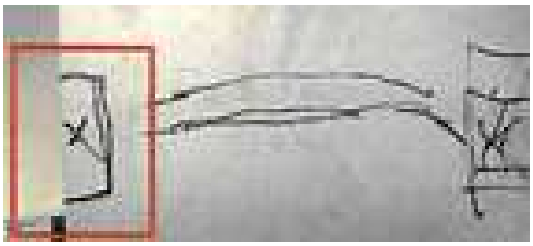

Figure 5.4 Region for sample preparation for surface examination

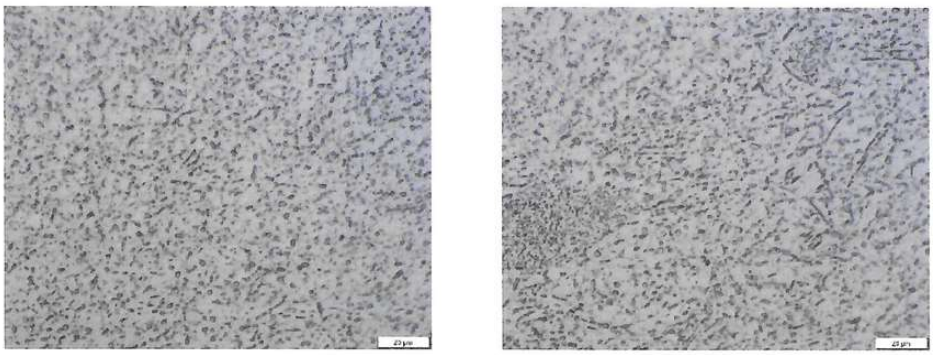

Figure 5.5 Microstructure images obtained from the surface area where the streak was observed

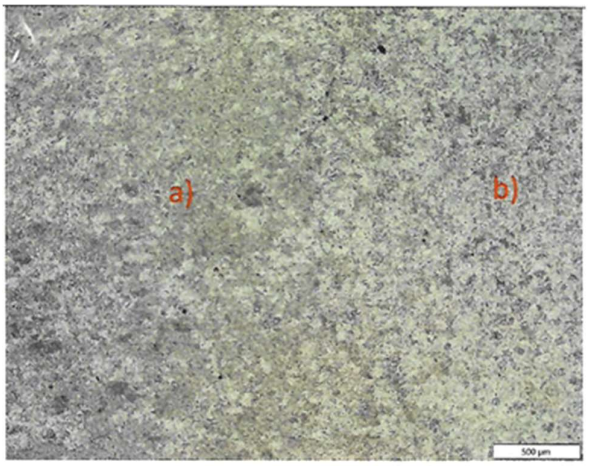

Figure 5.6 Region with varying phase density a) region with higher phase fraction, b) region with lower phase fraction

Upon microstructural examination of the marked region after macro etching, a variation in the density of phases was observed in the indicated area. Consequently, when the phase fraction was calculated based on the high-magnification images, as shown in Table 5.1, a difference of 5.21% was observed.

In the N2 sample, a clear stress flow structure can be observed as a result of forging. Macrostructure analysis did not reveal any macrostructural defects.

Table 5.1 Phase fraction of particle area

Segregation Region	Particle area fraction
Dense Region	22.07 %
Less Dense Region	16.85 %

Figure 5.7 Stress flow surface after etching for N2 sample

5.2 SEM - EDS Phase Analysis

In the SEM-EDS analysis of the Inconel 718 alloy microstructure sample, phases such as niobium-rich precipitates, niobium carbide, and titanium nitride were identified,

exhibiting a wide distribution throughout the microstructure. They are shown in Figures 5.8 and 5.9.

These phases present in the microstructure are believed to be primary precipitates that remain in the structure after solution treatment and aging heat treatment, or that have partially dissolved in the matrix and re-precipitated as phases depending on element diffusion during the aging heat treatment.

Figure 5.8 General appearance of the phases present in the microstructure.

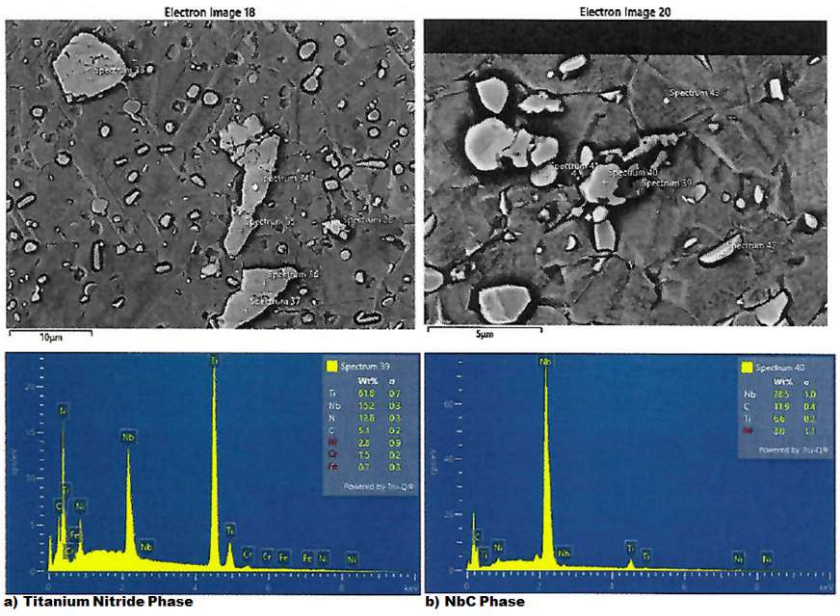

Figure 5.9 SEM image of (a) titanium nitride and (b) niobium carbide phases present in the microstructure

SEM-EDS analysis was conducted on the widely observed precipitates in the microstructure, which are generally spherical or block-like in shape. Two different phases with distinct compositions and sizes were identified. The first phase, depicted in Figure 5.10 and Table 5.2, is a larger-sized (Spectrum 17-18) spherical phase with a high niobium content. The SEM-EDS results pertaining to this phase are provided below.

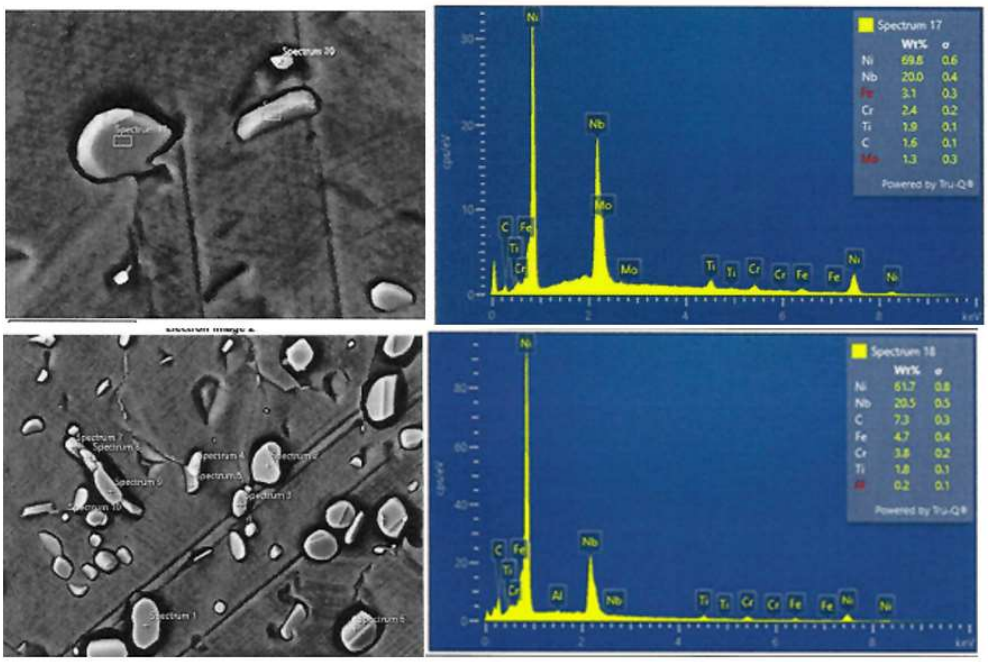

Figure 5.10 SEM images and elemental results of niobium-rich phases formed during casting

Table 5.2 Percentage and atomic EDS analysis of the niobium-rich phase

Spektrum 2	Atomic Percentage (%)
C	10.97
Ti	2.25
Cr	2.52
Fe	3.00
Ni	68.05
Nb	13.21
Total	100

In the EDS analysis, while the weight percentage analysis of the elements indicates a high content of niobium (approximately 21%), the atomic percentages reveal a ratio of approximately 1:3, with nickel accounting for 68.05% and niobium for 13.21%. The XRD analysis showed a diffraction peak at 2-theta 42°, suggesting that this phase could

be the gamma double prime phase, which is the main strengthening phase in the aged state of IN718 with a body-centered tetragonal structure composed of Nb and Ni.

The SEM-EDS values for the smaller spherical phase identified in the microstructure are provided in Figure 5.11.

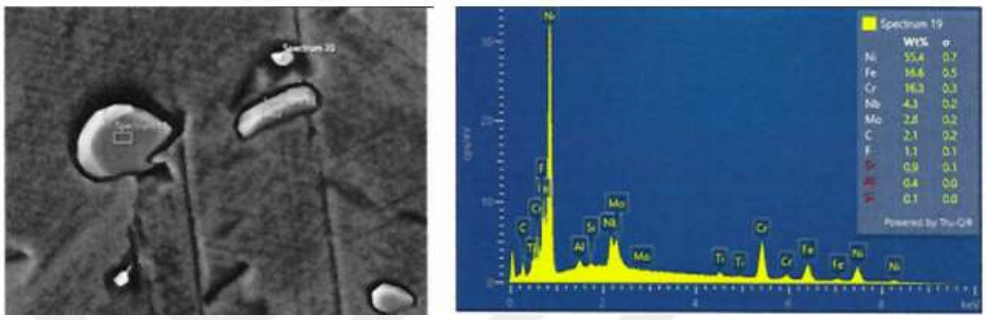

Figure 5.11 SEM-EDS analysis of the smaller-sized phase (Spectrum 19) compared to the other structure

This smaller-sized phase exhibits a higher content of iron and chromium in its elemental composition compared to the other phase. The element distribution and chemical composition values of this phase align with the percentage composition of the delta phase formed during solidification, as reported in the literature.

5.3 XRD Analysis

Six major peaks were recorded during the analysis. When these peaks were matched with appropriate patterns, it was interpreted that the phases present in the matrix, which is the YMK crystal structure, could be the gamma phase, and the phases present in the HMT crystal structure could be the gamma double prime phases. Sequentially, these peaks are shown in Table 5.3 and Figures 5.12, 5.13, 5.14.

When the major peaks obtained from the XRD analysis were matched with appropriate patterns, it was interpreted that the phases present in the matrix with an FCC crystal structure could be the gamma phase, while the phases in the BCT crystal structure could be the gamma double prime phases. Similarly, in the XRD analysis of the microstructure of SLM-produced Inconel 718, it was determined that, after heat treatment, delta (δ) and gamma double prime (γ") phases precipitated at the grain

boundaries, thereby strengthening the material properties. In the study conducted by Ergin et al., the presence of the gamma phase and carbide phases was identified in Inconel 718 superalloy produced by electric current activated sintering, while Vikram and colleagues examined the formation and distribution of phases in SLM-produced Inconel 718 and demonstrated the significant effects of these phases on mechanical performance. These studies confirm that the results obtained in this thesis are consistent with findings in the literature, showing that the formation of these phases has a reliable impact on the mechanical properties of the material [35-36].

Table 5.3 XRD peak list

No	2-theta (deg)	d (ang.)	Height (counts)	FWHM (deg)
1	42.786 (8)	2.112 (4)	4003 (63)	0.138 (9)
2	43.521 (2)	2.078 (10)	23156 (152)	0.135 (3)
3	50.625 (19)	1.801 (6)	4038 (64)	0.401 (14)
4	74.544 (12)	1.272 (17)	2866 (54)	0.370 (3)
5	90.492 (9)	1.085 (8)	1671 (41)	0.374 (19)
6	95.810 (4)	1.038 (3)	245 (16)	0.210 (10)

Phase 1 is austenite with the chemical formula Fe0.49 Cr0.29 Ni0.16 C0.06. The space group is Fm-3M (225) and the crystal system is cubic. Potential austenite phase showing diffraction peaks at 2-theta angles of 43.58°, 50.79°, 74.70°, 90.70°, and 95.97° in XRD analysis.

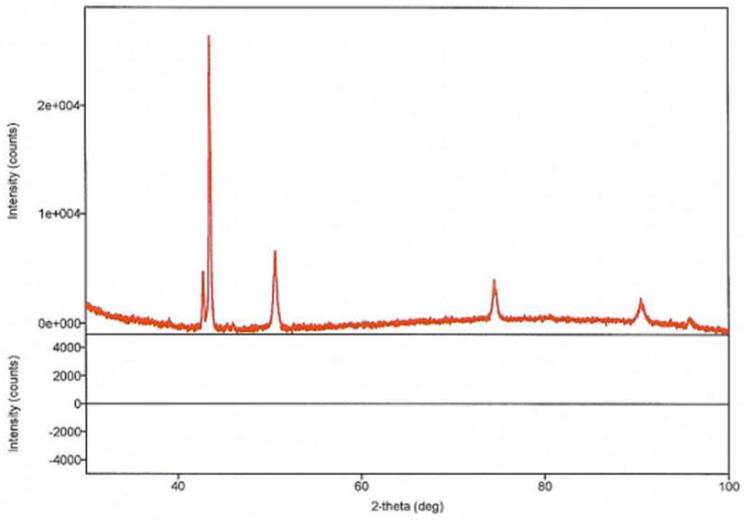

Figure 5.12 X-ray diffraction pattern of the IN718 microstructure sample

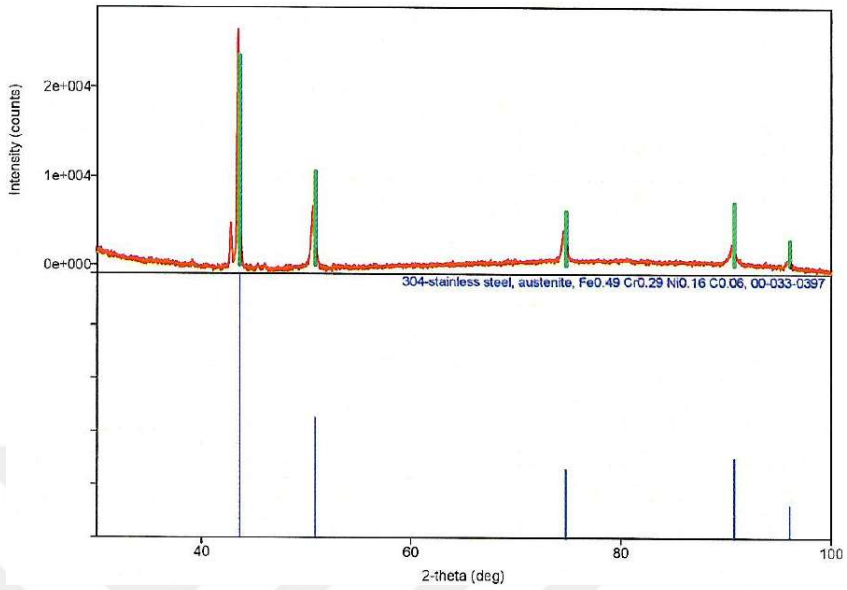

Figure 5.13 Potential austenite phase showing diffraction peaks in XRD analysis

Phase 2 is nickel niobium with the chemical formula NbNi. The space group is I4/mmm (139) and the crystal system is tetragonal.

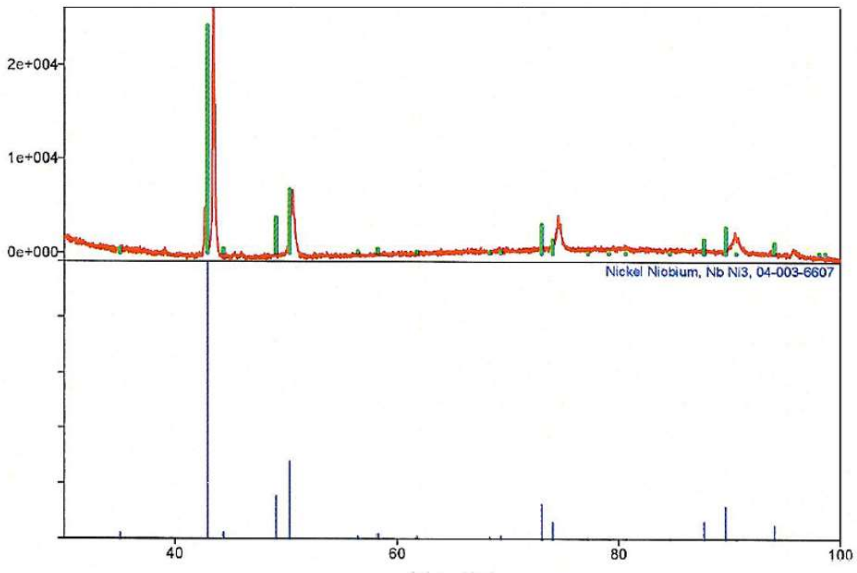

Figure 5.14 Possible gamma double prime phase showing a diffraction peak at 2-theta 42.91 degrees in XRD analysis

5.4 Grain Size Analysis

Following the acquisition of microstructure images, the calculation of average grain size for the samples was performed using the "Cross and Circles Grains Intercept" method. According to ASTM E112 standards, calculations were conducted using the digital image analyzer, determining the grain size number (G), average intercept length (µm), average intercept count, and intercept count per unit length (1/mm) for each sample. The images of the samples are shown in Figures 5.15, 5.16, 5.17, and 5.18, respectively. The average sizes are provided in Tables 5.4, 5.5, 5.6, and 5.7, respectively.

N1Size Cross-Section:

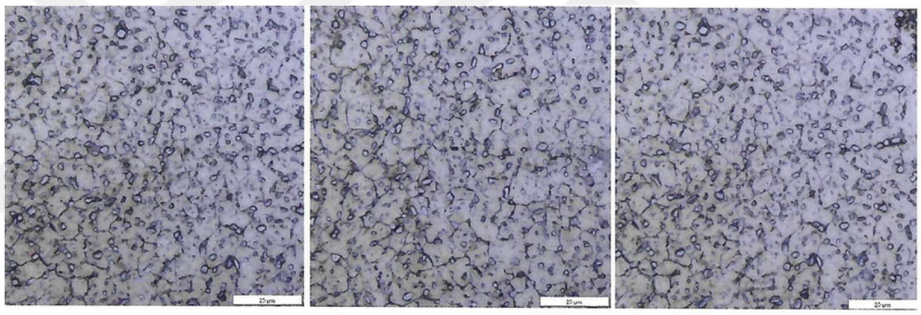

Figure 5.15 N1CS-1, N1CS-2, N1CS-3

Table 5.4 Average grain size

Sample	N1CS-1	N1CS-2	N1CS-3
Grain Size Number	11.53	10.17	11.03
Mean lntercept Length (µm)	5.89	9.43	7.00
Average Number of lntercepts	120.00	75.00	101.00
Number of lntercepts per Unit Length (1/mm)	169.72	106.07	142.84

N1Cross Section:

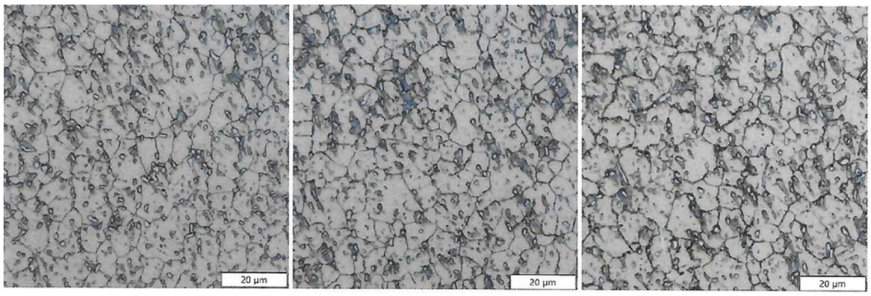

Figure 5.16 N1EN-1, N1EN-2, N1EN-3

Table 5.5 Average grain size of the specimens

Sample	N1EN-1	N1EN-2	N1EN-3
Grain Size Number	10.92	11.00	10.94
Mean lntercept Length (µm)	7.19	7.07	7.21
Average Number of lntercepts	99.00	100.00	98.00
Number of lntercepts per Unit Length (1/mm)	128.58	141.43	138.60

N2 Cross Section Length:

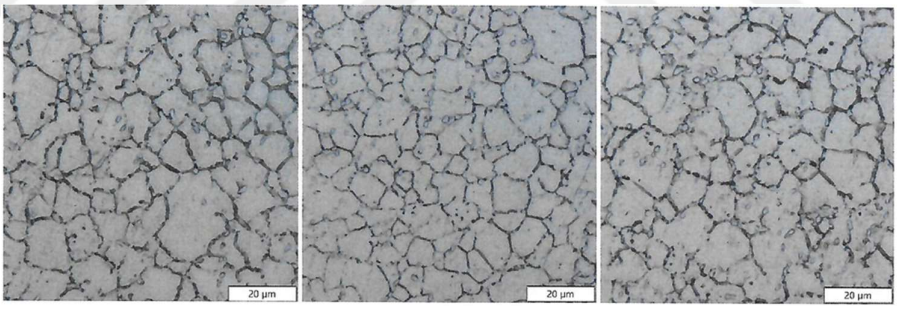

Figure 5.17 N2CROSS-1, N2CROSS-2, N2CROSS-3

Table 5.6 Average grain size

Sample	N2CROSS-1	N2CROSS-2	N2CROSS-3
Grain Size Number	10.63	10.88	10.36
Mean lntercept Length (µm)	8.03	6.31	8.84
Average Number of lntercepts	88.00	96.00	80.00
Number of lntercepts per Unit Length (1/mm)	124.46	135.77	113.14

N3 Cross Section:

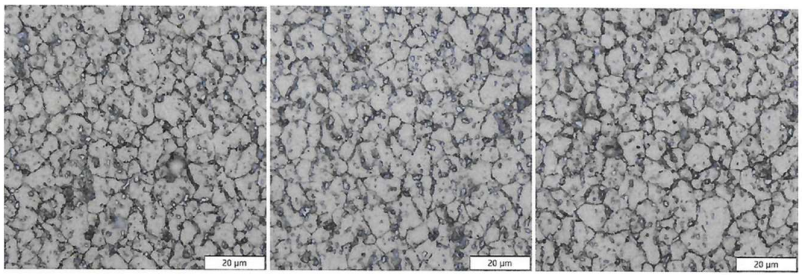

Figure 5.18 N3CROSS-1, N3CROSS-2, N3CROSS-3

Table 5.7 Average grain size

Sample	N3 EN-1	N3 EN-2	N3 EN-3
Grain Size Number	11.48	11.33	11.11
Mean lntercept Length (μm)	5.99	6.31	6.80
Average Number of lntercepts	118.00	112.00	104.00
Number of lntercepts per Unit Length (1/mm)	166.89	158.40	147.09

5.5 Ala Grain Size Measurement

When comparing the microstructure images of the current sample with the ALA grain size analysis specified in ASTM E930, it can be observed that the desired. Inconel 718 alloy samples exhibit a homogeneously distributed equiaxed grain structure across the surface and do not meet the conditions required for ALA grain size calculation according to ASTM E930. Figure 5.19 shows the following: "a)" at 125x magnification, where the ALA condition can be graded according to ASTM E930; "b)" at 100x magnification, depicting a bimodal condition where the microstructure does not contain ALA grains; and "c)" the most representative microstructure image of the samples.

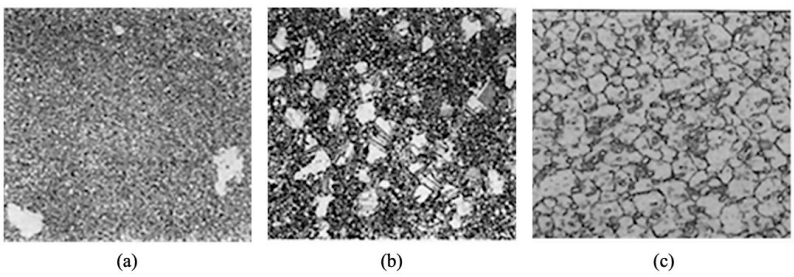

Figure 5.19 a) Microstructure image showing the measurable extent for ALA grain size analysis according to ASTM E930. b) Microstructure image showing the absence of ALA grains in the standard reference

5.6 Mechanical Tests Results

The results from the tensile tests at both room and elevated temperatures are presented in Tables 5.8, 5.9 and 5.10.

Table 5.8 Tensile test results at room temperature

	Yield (MPa)	UTS (MPa)	Elongation (%)	RA (%)
RT1	1136	1413	12.2	20
RT2	1161	1432	18.6	34
RT3	1121	1421	16.0	23
RT4	1128	1399	14.0	22
Mean	1136	1416	15.2	25
STD	17	14	2.7	6

Stress rupture tests were conducted in accordance with ASTM E292 using ATS 2330 creep testing machines at a temperature of 650°C and a stress level of 689 MPa. For the SR1 sample, the stress was increased by 34.5 MPa every 8 hours after 23 hours. The SR2 sample was stopped after 25 hours, and the elongation percentage was measured. The rupture time, rupture area, and elongation results for the stress rupture tests are presented in Table 5.11.

When examining the mechanical test results, it was observed that the compressive strength and hardness values of the Inconel 718 samples are in alignment with similar studies in the literature that utilize Spark Plasma Sintering (SPS) for producing Inconel 718 alloy. For instance, in the study conducted by Yan and colleagues, compressive strength values of 1349 MPa and hardness of 3.71 GPa were reported after solution treatment and aging, which are consistent with the strengthening effects observed in this study's results [37].

Table 5.9 High temperature (400°C) tensile test results

	Yield (MPa)	UTS (MPa)	Elongation (%)	RA (%)
HT1	994	1290	15.5	27
HT2	1011	1260	14.7	20
HT3	1030	1275	14.4	20
HT4	1028	1277	18.1	23
Mean	1016	1275	15.7	23
STD	17	12	1.7	3

Table 5.10 High temperature (650°C) tensile test results

	Yield (MPa)	UTS (MPa)	Elongation (%)	RA (%)
HT5	955	1158	20.9	59
HT6	970	1162	20.7	46
HT7	932	1136	21.5	44
HT8	954	1148	32.8	57
Mean	953	1151	24	51
STD	16	12	5.9	8

Table 5.11 Stress rupture test results

Sample	SR1 (NOTCH-STEP)	SR2 (NOTCH)
Test Temperature (°C)	650	650
Applied Stress (MPa)	689	689
Rupture Life (hr)	38:42	25:35
Elongation % in 4D	20.71	1.78
Rupture Location	In gage	-

CHAPTER 6

CONCLUSIONS

These results are based on mechanical tests conducted on Inconel 718 superalloy samples, performed in accordance with ASTM standards. These tests have been compared with relevant literature studies, including ALA grain size analysis and high-temperature stress rupture tests. For the ALA grain size analysis, samples that did not meet the criteria specified in the ASTM E930 standard were used. As a result, grain size calculations according to this standard could not be performed.

Tensile tests were conducted at different temperatures-room temperature, 400°C, and 650°C following the respective ASTM standards. The results of these tests, which are presented in the table, show consistency with similar studies reported in the literature. This alignment suggests that the outcomes of these tests are reliable and comparable to existing data.

Additionally, high-temperature stress rupture tests were performed at 650°C and a stress level of 689 MPa. The results of these tests are also included in the table and align well with literature studies. These high-temperature stress rupture tests provide valuable information on the performance of Inconel 718 under extreme conditions, contributing to a deeper understanding of the material's high-temperature stress resistance.

Overall, the findings are consistent with literature studies and offer valuable data for assessing the mechanical properties and high-temperature stress resistance of Inconel 718 superalloy. These tests establish a crucial foundation for understanding the alloy's performance under various temperature conditions and evaluating its suitability for high-temperature applications.

6.1. Future Works

Future research could focus on expanding high-temperature stress rupture tests to include a wider range of stress levels and temperatures, providing a more thorough

evaluation of Inconel 718's performance. Additionally, further investigation into the alloy's microstructure using advanced techniques like electron microscopy could reveal insights into the mechanisms affecting its properties. Exploring different heat treatment processes and their impact on the alloy's characteristics could also optimize its performance for specific applications. Lastly, integrating computational modeling with experimental data could enhance predictive capabilities and guide the development of more durable components.

REFERENCES

[1] Sims, C. T., Stoloff, N. S., & Hagel, W. C. Superalloys II: High-temperature materials for aerospace and industrial power. Wiley, 1987.

[2] Reed, R. C. The Superalloys: Fundamentals and Applications. Cambridge University Press, 2006.

[3] Pollock, T. M., & Tin, S. "Nickel-based superalloys for advanced turbine engines: Chemistry, microstructure and properties". Journal of Propulsion and Power, 22(2), 361-374, 2006.

[4] Ridhwan, J., Hamzah, E., Effendy, H., Selamat, M., & Zulfattah, Z. "Effect of Cooling Rate on the Microstructures and Hardness of Fe-Ni-Cr Superalloy". Journal of Mechanical Engineering and Technology, 5(1), 45-57, 2013.

[5] Ridhwan, J., Hamzah, E., Effendy, H., Selamat, M., & Zulfattah, Z. "Effect of Cooling Rate on the Microstructures and Hardness of Fe-Ni-Cr Superalloy". Journal of Mechanical Engineering and Technology, 5(1), 45-57, 2013.

[6] Zhao, X., Dang, Y., Yin, H., Lu, J., Yuan, Y., Yang, Z., & Yan, J. "Effect of heat treatment on the microstructure of a Ni–Fe based superalloy for advanced ultrasupercritical power plant applications". Progress in Natural Science: Materials International, 26, 204-209, 2016.

[7] Topuz, S. Effect of alloying elements and heat treatment on fatigue crack growth behavior of Fe-Ni-based superalloys / Alaşım elementleri ve ısıl işlemin Fe-Ni esaslı süperalaşımların yorulma çatlağı ilerlemesi tavrı üzerindeki etkisi (Yüksek Lisans Tezi). Orta Doğu Teknik Üniversitesi, Fen Bilimleri Enstitüsü, Metalurji ve Malzeme Mühendisliği Ana Bilim Dalı, 2022.

[8] Kazantseva, N. V., Stepanova, N. N., & Rigmant, M. B. Superalloys Analysis and Control of Failure Process. CRC Press, 2019.

[9] Davis, J. R. (Ed.). Heat-resistant Materials. ASM International, 1997.

[10] Eriş, R. Design and development of high temperature nickel-based superalloys / Yüksek sıcaklık uygulamalarında kullanılan nikel esaslı süper alaşımların tasarımı ve geliştirilmesi (Yüksek Lisans Tezi). Orta Doğu Teknik Üniversitesi, Fen Bilimleri Enstitüsü, Metalurji ve Malzeme Mühendisliği Ana Bilim Dalı, 2017.

[11] Pollock, T. M., & Tin, S. "Nickel-based superalloys for advanced turbine engines: Chemistry, microstructure, and properties". Journal of Propulsion and Power, 22(2), 361-374, 2006.

[12] MAN Energy Solutions. Chemical Reactors. Retrieved August 12, 2024, from https://www.man-es.com/process-industry/products/chemical-reactors adresinden erişildi.

[13] Wang, Q., Ma, N., & Watanabe, M. "Microstructure characteristics of warm spray additively manufactured Inconel 718 superalloys and correlation with mechanical performance". Materials Letters, 341, 134230, 2023.

[14] Thakur, A., & Gangopadhyay, S. "State-of-the-art in surface integrity in machining of nickel-based super alloys". International Journal of Machine Tools and Manufacture, 100, 25-54, 2016.

[15] Yin, Q., Liu, Z., Wang, B., Song, Q., & Cai, Y. "Recent progress of machinability and surface integrity for mechanical machining Inconel 718: a review". The International Journal of Advanced Manufacturing Technology, 109, 215-245, 2020.

[16] Kumar, A., & Rao, K. R. "Applications and properties of Inconel 718: A comprehensive review". Journal of Materials Science & Technology, 35(5), 1025-1042, 2019. doi:10.1016/j.jmst.2018.09.020.

[17] Smith, R. L., & Wang, Y. "High-temperature alloys for industrial applications: A focus on Inconel 718". International Journal of Aerospace Engineering, 2021, 1-15. doi:10.1155/2021/8886660.

[18] Groover, M. P. Fundamentals of Modern Manufacturing: Materials, Processes, and Systems (4th ed.). Hoboken, NJ: John Wiley & Sons, 2010.

[19] Taca, M., Daisa, D., & Constantinescu, D. M. "Influence of forging parameters on the structure and toughness of forged parts". Materials Today: Proceedings, 4(5, Part 1), 5969-5972, 2017.

[20] Semiatin, S. L., & Stutz, D. E. (Eds.). Forging: Technology and practice. Materials Park, OH: ASM International, 2004.

[21] Ghassemali, E. "Forging of metallic parts and structures". In P. J. Winkler (Ed.), Encyclopedia of Materials: Metals and Alloys. Elsevier, 2021.

[22] Li, Z., Zhang, C., Wang, C., & Huang, Y. "Research on material flow-stress behavior and the die-forging process for forged-steel brake discs for high-speed trains". MatTech, 55(6), 871-876, 2021.

[23] Liu, B., Hui, W., & Zhao, X. "Effect of vanadium on fatigue performance of a bainitic forging steel". International Journal of Fatigue, 167(Part B), 107398, 2023.

[24] Hawryluk, M., Gronostajski, Z., & Suliga, M. "An integrated vision control system for the evaluation of the shape-dimensional accuracy and quality of valve forgings used in motor truck engines". Measurement, 210, 112541, 2023.

[25] Kim, D. H., Lee, H. C., & Kim, K. H. "Estimation of die service life against plastic deformation and wear during hot forging processes". Journal of Materials Processing Technology, 166(3), 372-380, 2005.

[26] Padap, A. K., Chaudhari, G. P., Nath, S. K., et al. Mater. Sci. Eng. A, 527, 110–117, 2009. https://doi.org/10.1016/j.msea.2009.08.066.

[27] Feng, W., Jia, X., & Gao, M. "Material flow characteristics and deformation law during dual directional hot forging of the steel-aluminium spur gear". Procedia Manufacturing, 50, 425-428, 2020.

[28] Gudmundsson, S. "Chapter 5: Aircraft Structural Layout". In General Aviation Aircraft Design (Second Edition) (pp. 113-146), 2022.

[29] Arulmani, L., Shridharmurthy, H. N., & Madara, S. R. "Hot powder forging behavior analysis of sintered AISI 8740 PM steels for automotive application". Materials Today: Proceedings, 28(Part 2), 1068-1072, 2020.

[30] Pandya, V. A., & George, P. M. "Analysis of die stress and forging force for DIN 1.2714 die material during closed die forging of anchor shackle". Materials Today: Proceedings, 45(Part 6), 4695-4701, 2021.

[31] Yin, J., Hu, R., & Shu, X. "Closed-die forging process of copper alloy valve body: finite element simulation and experiments". Journal of Materials Research and Technology, 10(January–February), 1339-1347, 2021.

[32] Pc, S. "Multi directional forging: an advanced deforming technique for severe plastic deformation". In Advanced Welding and Deforming (pp. 529-556). Elsevier, 2021. https://doi.org/10.1016/B978-0-12-822049-8.00017-7.

[33] Kaufman, M., & Scholl, C. J. In E. A. Loria (Ed.), Superalloy 718—Metallurgy and Applications. TMS, Warrendale, PA, 1989, p. 189.

[34] Totten, G. E. Handbook of Metallurgical Process Design. CRC Press, 2004.

[35] Ergin, N., Ozdemir, O., Demirkiran, S., Sen, S., & Sen, U. Synthesis of Inconel 718 superalloy by electric current activated sintering. Acta Physica Polonica A, 127(4), 1100-1102. 2015. https://doi.org/10.12693/APhysPolA.127.1100.

[36] Vikram, R.J., Singh, A., & Suwas, S. Effect of heat treatment on the modification of microstructure of selective laser melted (SLM) IN718 and its consequences on mechanical behavior. Journal of Materials Research, 35(6), 1109-1123. 2020. https://doi.org/10.1557/jmr.2020.129.

[37] Yan, S., Wang, Q., Chen, X., Zhang, C., & Cui, G. Fabrication of highly compact Inconel 718 alloy by spark plasma sintering and solution treatment followed by aging. Vacuum, 163, 194-203. 2019. https://doi.org/10.1016/j.vacuum.2019.01.048